Production and characterization of iridium oxide films by ultrasonic chemical spray pyrolysis

O. GENÇYILMAZ[a*], F. ATAY[b], İ. AKYÜZ[b]
[a] Çankırı Karatekin University, Çankırı, 18100, Turkey
[b] Eskişehir Osmangazi University, Eskişehir, 26480, Turkey

Iridium oxide films were deposited onto glass substrate at 300±5 ºC by using ultrasonic chemical spray pyrolysis technique. The as-deposited films were annealed at 600 ºC in air medium for 3 h. The effects of anneal on structural, optical, morphological and electrical properties was studied. Effects of annealed iridium oxide on the crystalline nature, morphological, optical and electrical properties of the deposited films were analyzed by using X-ray diffraction, atomic force microscopy, UV-visible spectrophotometer and two-probe method, respectively. The X-ray diffraction studies showed that unannealed iridium oxide films were non-crystalline phase (Ir_2O_3). At annealing temperature of 600 ºC for 3 h, the films were fully transformed to polycrystalline phase of IrO_2. Also, the room temperature electrical resistivity of these films decreased and transmittance values increased with annealing process.

(Received January 22, 2014; accepted March 19, 2015)

Keywords: Iridium oxide, Spectroscopic ellipsometry, X-ray diffraction, Atomic force microscopy, Two-probe technique

1. Introduction

The transition metal oxides are great interest these last years because of the various properties that they exhibit [1]. Among these metal oxides, iridium oxide are nominated as a versatile candidate due to usability in many technological applications such as optical information storage [2], catalyst for O_2 evolution [3], photo electrolysis [4], electrochromic device [5], pH sensors [6], bio-sensor, H_2O_2 sensor, CO_2 sensor, etc. [7-9]. Iridium oxide is one of the versatile oxide materials among the transition metal oxides that exhibit metallic resistivity at room-temperature. It crystallizes in the tetragonal rutile structure and has been used for many applications due to its attractive electrical, optical, and electrochemical properties [10, 11]. Ir has low oxygen permeability, high chemical stability, and good electric conductivity [12-14]. Moreover, the oxide of Ir is also a good conductive oxide (IrO_2), and the formation of IrO_2 can prevent the permeability of oxygen [15]. Iridium oxide (IrO_2) films have been prepared using different physical and chemical techniques such as electro deposition [16], sol-gel processing [17], a sputtering method [18, 19], anodic oxidation [20], thermal oxidation [5 20], spray pyrolysis [21, 22], pulsed laser deposition [22-25], chemical vapor deposition [26]. Recently, many researchers are interested in iridium oxide films in connection with the electrochromism. The electorchromic studies of these materials could be applied to the large area display and smart window application. Especially, anodic oxidation and reactive sputtering techniques are largely used to produce for iridium oxide. But, in anodic oxidation technique, finite electrical conductivity of transparent electrode and limits the uniform growth of oxide. The reactive sputtering technique is more attractive due to it is a dry process. However this technique has limitation in obtaining large area film. So, we would be interesting to study iridium oxide film deposited but ultrasonic spray pyrolysis, which is economic, an effective technique and has potential to growth good quality large area thin film coating [20,22,27].

Most of these techniques are either not favorable or too expensive for industrial applications. In contrast, the spray pyrolysis technique has been only rarely used although this process presents many advantages: (i) it includes high deposition rates (ii) it is a low-cost and simple technique, (iii) it allows the possibility of obtaining films with a large area, (iv) it is not require to vacuum, (v) it is reproducible, (vi) it is non-planer geometries. In the present investigation, iridium oxide films were deposited on glass substrates at 300 °C substrate temperatures by means of UCSP technique and we reported the correlation between structural, optical, electrical and morphological properties of iridium oxide films.

2. Experimental details

Iridium oxide films were deposited using the ultrasonic chemical spray pyrolysis technique (UCSP) at a substrate temperature of 300±5 °C. The substrate temperature was measured using a thermocouple embedded in the substrate holder beneath the substrate mounting area. A homogeneous solution was prepared by dissolving iridium chloride ($IrCl_3.3H_2O$) (0.01M) in distilled water. Some drops of acetic acid (CH_3COOH) were added to obtain a clear solution, which was stirred during 15 min. The glass substrates were cleaned in ethanol, rinsed in distilled water by ultrasonic bath and subsequently dried before deposition. The spray nozzle

and the substrate were kept at a distance of 30 cm from and the growth was performed with a spray rate of about 5 ml/min. Compressed air was used as the carrier gas with the airflow rate maintained at 1 bar. The annealing was carried out at 600 °C for 3 h in air ambient. The aqueous iridium chloride solution after being sprayed through an atomizer onto the preheated glass substrate, was under went pyrolytic decomposition, forming there by a thin solid film. The chemical reaction that took place as follow: *(Substrate temperature 300 ˚C)*

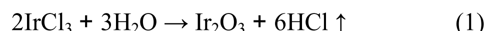

$$2IrCl_3 + 3H_2O \rightarrow Ir_2O_3 + 6HCl\uparrow \quad (1)$$

The as-deposited samples after annealing transform into IrO_2 according to the following:
(Annealing temperature 600 ˚C)

$$Ir_2O_3 \rightarrow 2IrO_2 \quad (2)$$

The resulting films were found to be uniform, strongly adherent to substrate and blackish in color. The crystal structure of the as-deposited and annealed films was examined by X-ray diffractometer (XRD) with CuK_α radiation. The film thickness of samples was measured using the spectroscopic ellipsometry (SE). Optical transmission, absorbance and reflectance spectra of iridium oxide films were performed with a UV–VIS–NIR spectrophotometer over the wavelength range of 300–900 nm. In addition, optical characteristics of iridium oxide films including the absorption coefficient, energy gaps, optical constants and dielectric constants were investigated. Atom force microscopy (AFM) was used to measure the surface morphology and roughness of the films. Also, electrical resistivities of films were determined by a two-probe technique. These measurements were made using Hewlett Packard 4140B Model pA Meter/DC voltage source.

3. Results and discussion

3.1. X-ray diffraction studies

Rigaku X-ray diffractometer with CuK_α radiation between $20^\circ \leq 2\theta \leq 70^\circ$ was used for X-ray diffraction studies. Crystallinity levels of the films were investigated. The results of XRD for as-deposited iridium oxide films show that the film structure is non-crystalline phase. When the deposited films are annealed at 600 °C for 3 h in ambient air atmosphere, the amorphous films became polycrystalline. Fig. 1 shows XRD patterns of the as-deposited and annealed film. After annealing crystallinity of IrO_2 improves and become polycrystalline and Ir_2O_3 becomes polycrystalline IrO_2. The presence of the characteristic lines corresponding to (110), (111), (200) and (220), planes of IrO_2 are clearly shown in Fig. 1.

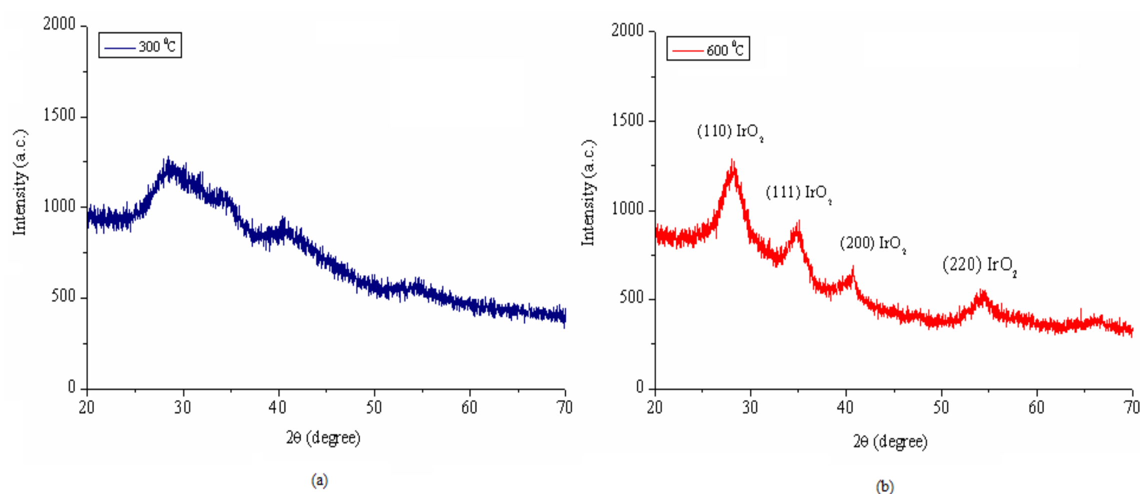

Fig. 1. XRD patterns of the (a) as-deposited and (b) annealed films.

3.2 Spectroscopic ellipsometry study

The thickness (*d*), refractive indices (*n*), extinction coefficient (*k*) and *Δ* parameters, dielectric constants (ε_1 and ε_2) of the iridium oxide films have been studied using PHE-102 spectroscopic ellipsometer (250–2300 nm). One of the most important techniques is SE, which has been found favorably for characterization of thin solid films and bulk materials, especially semiconductors. This technique is a non-destructive, powerful and accurate technique [28, 29] and is based on the polarized light [30]. In spectroscopic ellipsometry (SE) measurements, two parameters, *Ψ* and *Δ* are measured as a function of the wavelength (or photon energy) from a given sample. These two parameters are related to the optical and structural properties of the sample through the following expression,

$$\rho = \frac{R_p}{R_s} = tg\,\psi e^{(i\Delta)} \tag{3}$$

where R_p and R_s are the complex reflection coefficients for the light polarized parallel (p) and perpendicular (s) to the plane of incidence, respectively [31]. Cauchy–Urbach dispersion model was used to fit the experimental Δ parameters. In the Cauchy–Urbach dispersion model, the refractive index $n(\lambda)$ and the extinction coefficient $k(\lambda)$ as a function of the wavelength are given by,

$$n(\lambda) = A_n + \frac{B_n}{\lambda^2} + \frac{C_n}{\lambda^4} \qquad (\lambda) = A_k e^{B_k(E-E_b)} \tag{4}$$

where A_n, B_n, C_n, A_k and B_k are model parameters [32-34]. So, we performed our measurements between 1200 and 1600 nm wavelength range where the films have low absorption. A good fitting is achieved between the measured and calculated spectra. During the fitting process, first we varied the optical constants of iridium oxide and the best fitting was obtained from the 175-176 nm thicknesses. Δ spectra of iridium oxide films on glass substrates in the wavelength range of 1200–1600 nm are shown in Fig 2. According to Fig 2, good matching was achieved between the measured and calculated Δ spectra but small mismatch is observed at various wavelengths. We think that reasons of the mismatches in the Δ values, (i) films produced by USP have not absolutely uniform and homogeneous surfaces (ii) roughness, grain boundaries and morphology of the films, (iii) backside reflection of transparent glass substrates. Thicknesses, refractive indices and extinction coefficients of all films have been determined using these Δ spectra. These values and model parameters are given in Table 1.

Table 1. Thicknesses and some (SE) model parameters of iridium films.

Film	d (nm)	A_n	B_n $(nm)^2$	C_n $(nm)^4$	A_k	$B_k(eV)^{-1}$	MSE
IrO-300 °C	175	2.14	0.18	0.13	0.48	0.25	0.39
IrO-600 °C	176	2.19	0.18	0.12	0.26	0.25	0.30

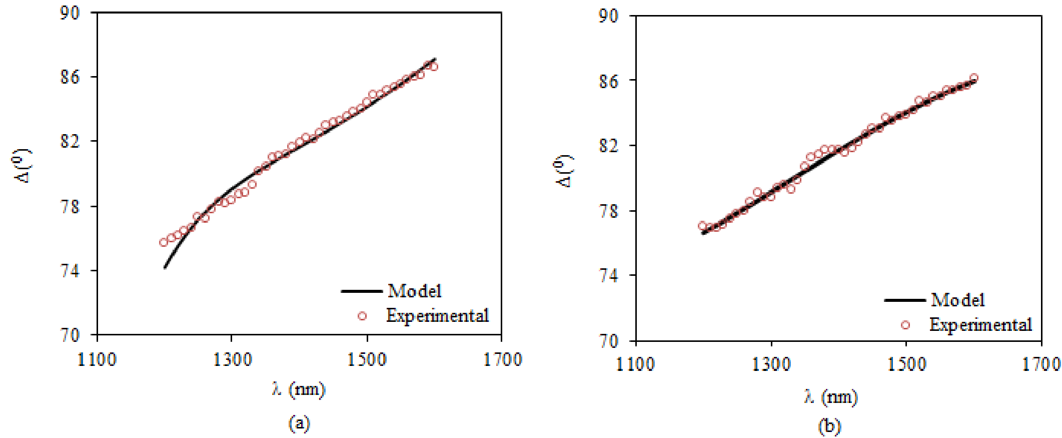

Fig. 2. SE spectra (a) as-deposited and (b) annealed of iridium oxide films.

Fig. 3 shows refractive index (n) and extinction coefficients (k) spectra of iridium oxide films which are derived from model fitting the experimental spectroscopic ellipsometric data. Refractive index values of the samples are nearly constant (~2.25–2.3) at long wavelengths. The extinction coefficient of a material is directly related to its absorption characteristic. As shown in Fig. 3, the k values are very small at long wavelengths where all films are nearly transparent. The real and imaginary parts of the dielectric constant can be given in the following form [35].

$$\varepsilon_1 = n^2 - k^2 \quad \text{and} \quad \varepsilon_2 = 2nk \tag{5}$$

Fig. 4 shows the dependences of ε_1 and ε_2 on photon energy. The real and imaginary parts follow the same pattern and it is seen that the values of real part are higher than imaginary parts. The almost stationary of the dielectric constant with photon energy indicates that some interactions between photons and electrons in the annealed films are produced more than as-deposited in this energy range.

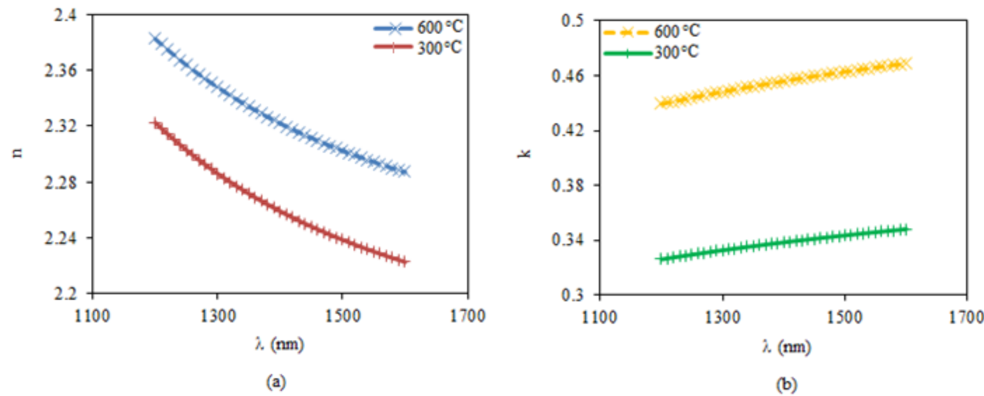

Fig. 3. (a) Refractive index (n) and (b) extinction coefficients (k) spectra of films.

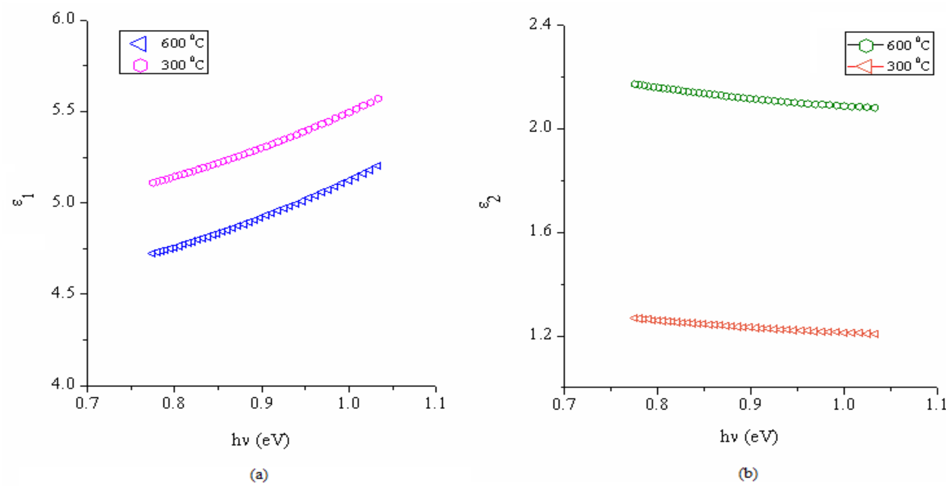

Fig. 4. The dielectric constant plots of the films: (a) real part and (b) imaginary part.

3.3 Optical studies

The optical properties were studied by UV-Visible (UV-Vis) spectrophotometer, which the model was Shimadzu UV-2550/UV-VIS-NIR spectrophotometer. Optical characterization iridium oxide films were performed by absorbance (A) and reflectance (R) spectra from 300 to 900 nm**.** The all spectra of films are presented in Fig 5. The properties of films changes with the annealing. Thus, the changes in the absorbance and reflectance take place. We think that decrease of reflectance results from the surface roughness, grain boundaries and morphology of the iridium oxide films as these properties affect the intensity of the reflected light. Because of this information, we can say that the unannealing, which has the highest average reflection value, has a uniform surface structure and lower roughness as compared with others.

The fundamental absorption edge of the films corresponds to electron transitions from valence band to conduction band and this edge can be used to calculate the optical band gap of films. In the direct transition, the absorption coefficient can be expressed by [36];

$$(\alpha h\nu) = A\ (h\nu - E_g)^1 \qquad (6)$$

where A is a constant, $h\nu$ is photon energy and E_g is the optical band. Fig 6 shows plots of $(\alpha h\nu)^2$ versus $h\nu$. The nature of plots suggests direct interband transition. The extrapolation of straight line portions to zero absorption coefficient ($\alpha = 0$), leads to the estimation of band gap energy values. The optical band gaps of the films were calculated from these plots and are given in Table 2.

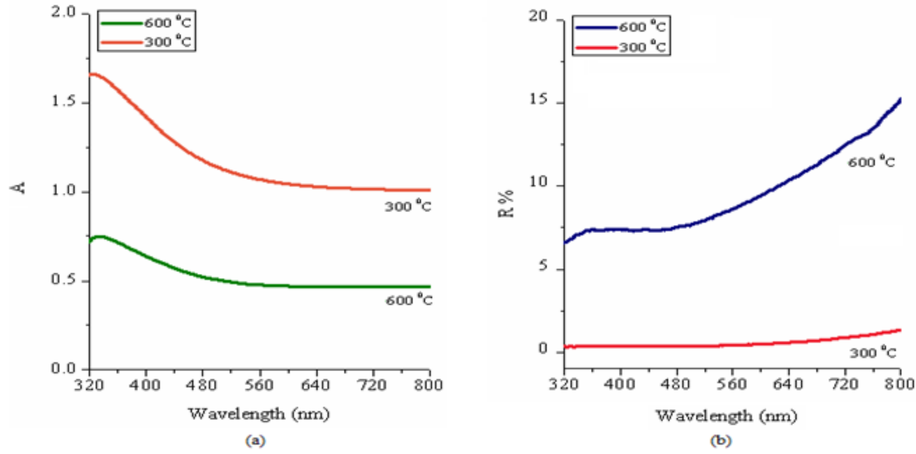

Fig. 5. Room temperature optical (a) A and (b) R ~ λ spectra of iridium oxide films.

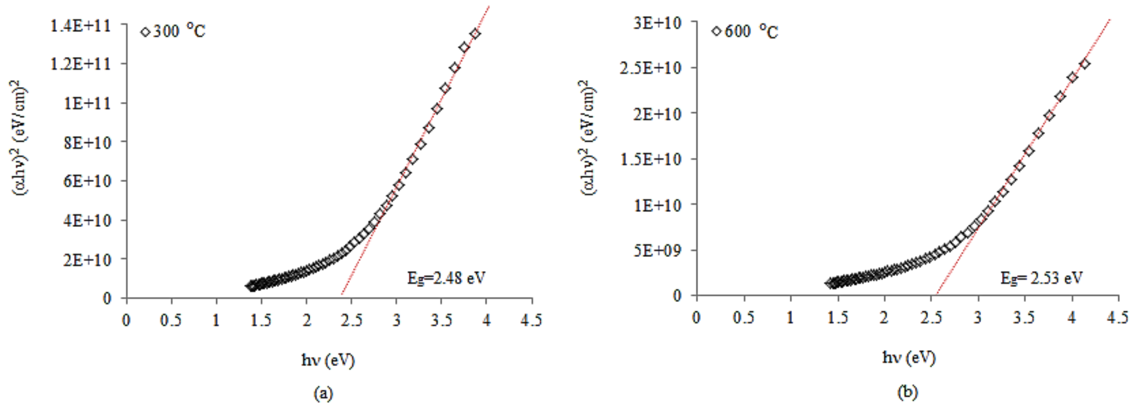

Fig. 6. The plots of $(\alpha h\nu)^2$ vs. photon energy of films: (a) as-deposited and (b) annealed of iridium oxide films.

The absorption edge can be determined from the exponential dependence of the absorption coefficient and it is determined as [37]

$$(\alpha h\nu) = \alpha_0 \exp (h\nu/E_u) \quad (7)$$

where α_0 is a constant and E_u is the Urbach energy. Plotting the dependence of $ln\alpha$ vs. $h\nu$ as shown in Fig. 7 should give a straight line.

The E_u values were calculated from the following relationship,

$$E_u=(d \ln \alpha / d h\nu)^{-1} \quad (8)$$

The steepness parameter, $\sigma = kT/E_u$; characterizing the broadening of the optical absorption edge due to electron phonon or exciton–phonon interactions [38] was also determined taking T=300 K and given in Table 2. E_u values change inversely with optical band gap. The refractive index dispersion of the compounds studied can be fitted by the Wemple–DiDomenico relationship. The dispersion plays an important role in the research for optical materials, because it is a significant factor in optical communication and in designing devices for spectral dispersion. The result of refractive index dispersion below the interband absorption edge corresponds to the fundamental electronic excitation spectrum. Thus, the refractive index is related to photon energy through the relationship [39, 40];

$$n^2-1 = E_0 E_d / [E_0^2-(h\nu)^2] \quad (9)$$

where E_o and E_d are single-oscillator constants. The values of E_o and E_d parameters are calculated by plotting $(n^2-1)^{-1}$ vs. $(h\nu)^2$ (Fig. 8) and these values given in Table 2. The parameter E_d is the oscillator strength or dispersion energy which is a measure of the strength of interband optical transitions. The oscillator energy E_o is an average energy gap. Furthermore, an approximate value of the optical band gap, E_g, can be obtained from the Wemple–Didomenico model. The optical band gap values, E_g, were also calculated from the Wemple–DiDomenico dispersion parameter, E_o, using $E_g \approx E_o/2$ relationship [41, 42]. The value of E_0 but the value of E_d decreases with annealing.

Table 2. Optical parameters of the iridium oxide films.

Film (IrO)	E_g (eV) (error ±1.8×10^{-5})	E_u (meV) (error ±3.2×10^{-4})	σ (error ±2.9×10^{-4})	E_o (eV) (error ±6.4×10^{-5})	E_d (eV) (error ±2.5×10^{-4})
300 °C	2.34	293.01	0.088	5.16	1.35
600 °C	2.09	329.06	0.079	5.28	1.15

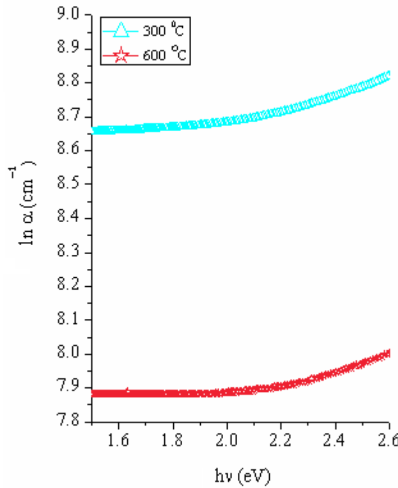

Fig. 7. The Urbach plots of the iridium oxide films.

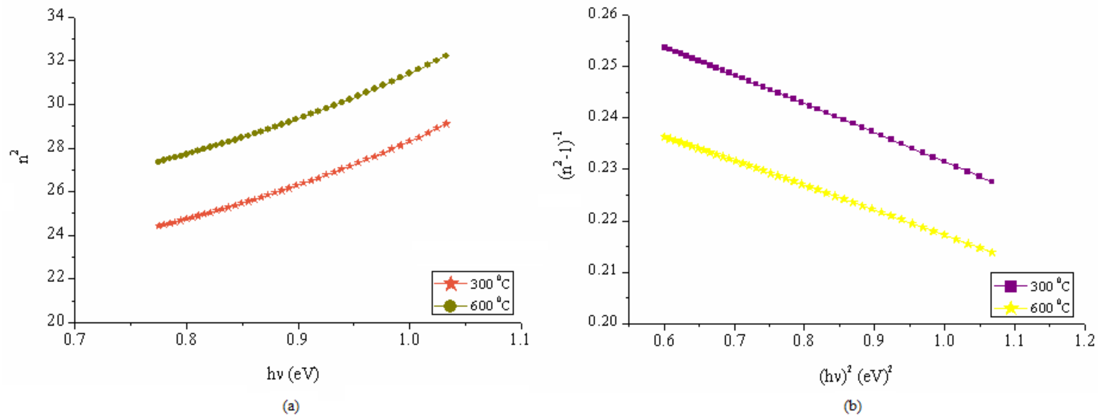

Fig. 8. The (a) n^2 vs. $(h\nu)^2$ and (b) $(n^2-1)^{-1}$ vs. $(h\nu)^2$ plots of the iridium oxide films.

3.4 Morphological study

Surface images of the iridium oxide films were investigated by Park System XE-70 AFM. The measurements were taken in non-contact mode, ~300 kHz frequency and 0.65 Hz scan rate in air at room temperature. Also, average (R_a) and root mean square (R_q, rms) roughness values were determined using XEI version 1.7.1 software. All the images were taken from an area of 5 µm × 5 µm. The roughness values belong to whole scanned area. Fig. 9 shows the AFM images of iridium oxide films. The surface morphology of the all films shows smooth, layer-by-layer and columnar surface. Some columnar constitution can be seen on the surface, which are superficial and might be the result of thermal shocks due to different thermal expansion coefficients of iridium oxide and glass substrates. R_a and R_q values of the all films are given in Table 3. It is clear that annealing affected the roughness values of iridium oxide films.

Table 3. R_q and R_a roughness values of iridium oxide films.

Film	R_a(nm)	R_q(nm)
IrO-300 °C	30	38
IrO-600 °C	19	27

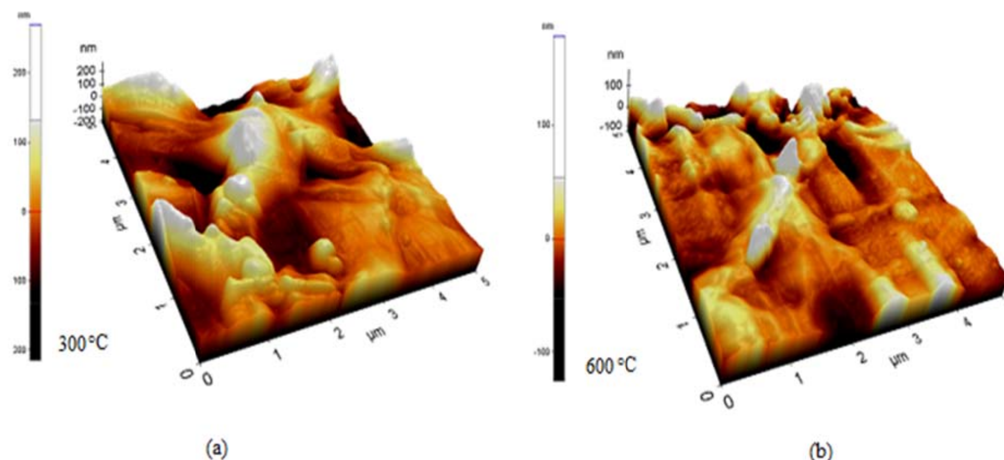

Fig. 9. AFM images of (a) as-deposited and (b) annealed of iridium oxide films.

3.5 Electrical study

The electrical resistivity values of the as-deposited and annealed films were studied by two-probe technique in the temperature range 25-445 °C. The room temperature electrical resistivity varies from 4.23×10^{-1} Ω cm for as-deposited film to 2.82×10^{-3} Ω cm for annealed film. Also, the electrical resistivity values of the films are between 4.23×10^{-1} Ω cm and 2.82×10^{-3} Ω cm which are lower than that of the results of the report given by Patil et al. [43]. Fig. 10(a) shows temperature dependence of resistivity for as-deposited film, which decays in the 25-445 °C. Fig. 10(b) shows temperature dependence of resistivity for annealed film. The resistivity of annealed film slightly increases with increase in temperature, which indicates that annealed film exhibits metallic like conductivity, elucidating transformation from semiconducting (Ir_2O_3) to metallic (IrO_2). Similar results are reported by Patil et al. [43] for electrical resistivities of iridium oxide films. In iridium oxide films this kind of transformation from semiconducting to metallic has been informed frequently. A semiconducting to metallic transition in iridium oxide films has been conceived to be due to the change in oxidation state of iridium (3^+ to 4^+) as a result which Fermi energy level E_f crosses the conduction band edge E_c [44,45].

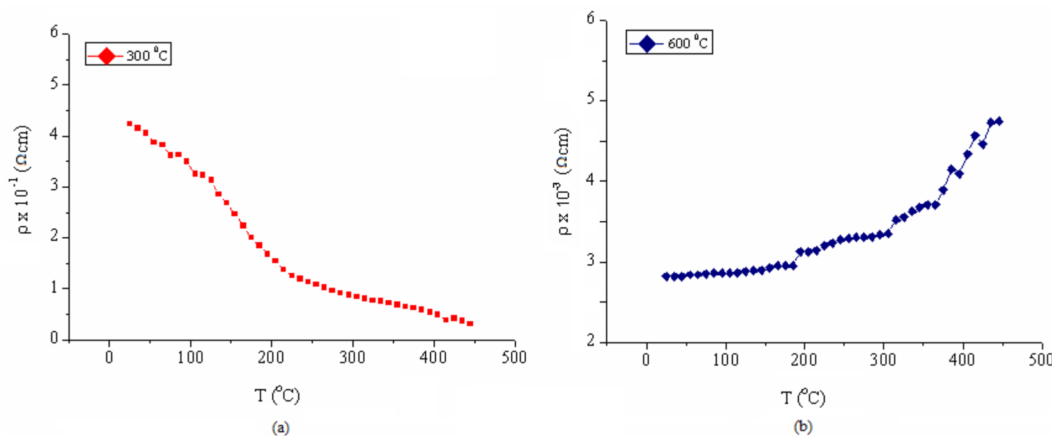

Fig. 10. Variation of electrical resistivity with temperature for (a) as-deposited and (b) annealed of iridium oxide films.

4. Conclusion

In this study, the structural, optical, surface and electrical properties of iridium oxide film deposited on glass substrates by ultrasonic chemical spray pyrolysis were studied. Iridium oxide films are polycrystalline annealed at 600 °C. Optical measurements show that the films have low transparency. Furthermore, the annealing process of iridium oxide films affects the refractive index, extinction coefficient, thickness and surface roughness of the films. AFM measurements show that the films became uniform as the annealing. The electrical resistivity of all the as-deposited and annealed samples was studied using two-probe technique. The as-deposited film behaves like semiconductor, whereas annealed film exhibited metallic behavior.

References

[1] C.N.R. Rao, B. Raveau Transition Metal Oxides, New York Wiley, (1995).
[2] S. Hacwood, G. Beni, M.A. Bosch, K. Kang, L.M. Schiavone, J.L. Shay, Phys. Rev. B **26**, 7073 (1982).
[3] D.N. Buckley, L.D. Burke, J. Chem. Soc. **1**, 2431 (1976).
[4] J.G. Posa, Electronics **53**, 39 (1980).
[5] G. Beni, J.L. Shay, Appl. Phys. Lett. **33**, 567 (1978).
[6] K.G. Kreider, M.J. Tarlov, J.P. Cline, Sens. Actuators, B, Chem. **28**, 167 (1995).
[7] J.V Dobson., P.R. Snodin, H.R. Thirsk, Electrochim. Acta **21**, 527 (1976).
[8] R.E. Abu, H. Elzanowska, A.S. Jhas, V. Birss, J. Electranal. Chem. **538**, 156 (2002).
[9] P. S. Patil, R.K. Kawar, S.B. Sadale, Applied Surface Science **249**, 367 (2005).
[10] M. L. Hitchman, S. Ramanathan, Anal. Chim. Acta **263**, 53 (1992).
[11] R.K. Kawar, P.S. Chigare, P.S. Patil, Appl. Surf. Sci. **206**, 90 (2003).
[12] J. Backholm, A. Azens, G.A. Niklasson, Sol. Energy Mater. Sol. Cells **90**, 414 (2006).
[13] J. Backholm, AE. vendano, A. Azens, G. de M. Azevedo, E Coronel. NG.A Iklasson, C.G. Granqvist, Solar Energy Materials & Solar Cells **92**, 91 (2008).
[14] S. Thanawala, D. G. Georgiev, R. J. Baird, Auner G., Thin Solid Film **515**, 7059 (2007).
[15] Y. Gong, C. Wang, Q. Shen, L. Zhang, Applied Surface Science **254**, 3921 (2008).
[16] K. Nomura, H. Ohta, A. Takagi, T. Kamiya, M. Hirano, H. Hosono, Nature **432**, 488 (2004).
[17] K. Nishio, Y. Watanabe, T. Tsuchiya, Thin Solid Films **350**, 96 (1999).
[18] M. I. Yanovskaya, I.E. Obvintseva, V.G. Kessler, B.S. Galyamov., S.I Kucheiko., R.R. Shifrina, N. Turova, Ya. Galyamov, J. Non-Cryst. Solids **124**, 155 (1990).
[19] M. Watanabe, Y. Koike, T. Yoshimura, K. Kiyota, Proc. Jpn. Disp. **83**, 372 (1983).
[20] R.K. Kawar, P.S. Chigare, P. S. Patil, Applied Surface Science **206**, 90 (2003).
[21] C. G. Granqvist, Handbook of Inorganic Electrochromic Materials, Amsterdam, Elsevier, 1995, (reprinted 2002).
[22] S.A. Mahmoud, S Al-Shomar.M, Physica B **404**, 2151 (2009).
[23] Y. X. Liu, H. Masumoto, T. Goto, Mater. Trans. **45**, 900 (2004).
[24] M. Galeazzi, C. Chen, J.L. Cohn, J.O Gundersen., Nucl. Instrum. Methods Phys. Res. A **520**, 293 (2004).
[25] D. Pergolesi, F. Gatti, L. Gastaldo, M.R. Gomes, S. Dussoni, R. Valle, P. Repetto, D. Marre´b, E. Bellingeri, Nucl. Instrum. Methods Phys. Res. A **520**, 311 (2004).
[26] Y.S. Huang, S.S. Lin, C.R. Huang, M.C. Lee, T.E. Dann, F.Z Chienn., Solid State Commun. **70**, 517 (1989).
[27] P.S. Patil, S.H. Mujawar, S.B. Sadale, H.P. Deshöukh, A.I. Inamdar, Mater. Chem. And Phys. **99**, 309 (2006).
[28] S.H. Wemple, M. DiDomenico, Phy. Rev. B **3**, 1338 (1971).
[29] M. Mansour, A.E. Naciri, L. Johann, S. Duguay, J.J. Grob, M. Stchakovsky, C Eypert., J. Phys. Chem. Solids **67**, 1291 (2006).
[30] A. Liu, J. Xue, X. Meng, J. Sun, Z. Huang, J. Chu, Appl. Surf. Sci. **254**, 5660 (2008).
[31] F. K. Shan, Z.F. Liu, G.X. Lıu, B.C. Shin, Y.S. Yu, S.Y. Kim, T.S. Kim, Journal of Korean Physical Society **44**, 1215 (2004).
[32] M. J. Khoshman, E.M. Kordesch, Journal of Non-Crystalline Solids **351**, 3334 (2005).
[33] Z. G. Hu, G.S. Wang, Z.M. Huang, J.H. Chu, Appl. Phys. **93**, 3811 (2003).
[34] R.M.A. Azam, N.M. Bashara, Ellipsometry and Polarized Light, North-Holland, New York, 1987.
[35] A.K. Wolaton, T.S. Moss, Proc. R. Soc. **81**, 5091 (1963).
[36] N. F. Mott, R. W. Gurney, Electronic Processes in Ionic Crystals, Oxford Univ. Press, London (1940).
[37] F. Urbach, Phys. Rev. **92**, 1324 (1953).
[38] H. Mahr, Phys. Rev. **125**, 1510 (1962).
[39] D. K. Goyal, G.K. Pribil, J.A. Woollam, A. Subramanian,Mater. Sci. Eng. B **149**, 26 (2008).
[40] M. DiDomenico, S.H. Wemple, J. Appl. Phys. **40**, 720 (1969).
[41] E. Marquez, A.M. Bernal-Oliva, J.M. Gonzalez-Leal, R. Pricto-Alcon, A. Ledesma, R. Jimenez-Garay, I. Martil, Mater. Chem. Phys. **60**, 231(1999).
[42] E. Marquez, P. Nagels, J.M. Gonzalez-Leal, A.M. Bernal- Oliva, E. Sleeckx, R. Callaerts, Vacuum **52**, 55 (1999).
[43] P.S. Patil, R.K. Kawar, S.B. Sadale, A.I. Inamdar, H.P. Deshmukh, Applied Surface Science **252**, 8371 (2006).
[44] R. Sanjnes, A. Aruchamy, F. Levy, Solid State Commun. **64**, 1740 (1987).
[45] S. Hackwood, A. H. Dayen, G. Beni, Phys. Rev. B **26**, 471 (1982).

*Corresponding author: eren_o@hotmail.com